COBEM 2023 27TH INTERNATIONAL CONGRESS OF MECHANICAL ENGENEERING

ABCM Brazilian Society of Mechanical Sciences and Engineering
27th ABCM International Congress of Mechanical Engineering
December 04-08, 2023, Florianópolis-SC, Brazil

COB-2023-0359
A COMPARISON STUDY BETWEEN HIGH-FIDELITY AND MID-FIDELITY MODELS OF CORONARY BLOOD FLOW SIMULATION

Amaury A. Santos
Alexandre M. S. Costa
Departamento de Engenharia Mecânica, Universidade Estadual de Maringá, Av Colombo 5790, Maringá, PR, Brasil
amaury.as@yahoo.com, amscosta@uem.br

L. A. Mansilla Alvarez
P. J. Blanco
National Laboratory for Scientific Computing, LNCC/MCTI, Av. Getúlio Vargas, 333, Petrópolis, RJ, Brasil
lalvarez@lncc.br, pjblanco@lncc.br

***Abstract**: Arterial circulation is an incredibly complex system, and understanding its flow dynamics is crucial for providing better treatments for cardiovascular diseases. Coronary flow simulation has become a significant research tool for studying fluid mechanics in coronary arteries. The development of numerical methods in Computational Fluid Dynamics (CFD) has allowed researchers to model and analyze complex flow patterns in the coronary network with unprecedented detail. CFD models can simulate the effects of various boundary conditions, the presence of atherosclerotic plaques, surgical interventions (e.g., stent placement), and physiological parameter effects (e.g., blood viscosity and shear stress). This study aims to compare the results of a high-fidelity model (Finite Volume Method, FVM) and a medium-fidelity numerical approach (Transversely Enriched Pipe Element Method, TEPEM). The medium-fidelity numerical strategy is positioned between low-fidelity and high-fidelity models to simulate fluid flow in tubular domains. While a high-fidelity model can provide detailed predictions, its application to clinical settings is prohibitively expensive. An in-house code was used to implement the medium-fidelity model (TEPEM), and a commercial solver (ANSYS FLUENT) was used to generate the high-fidelity model (FVM). As an initial study, both methods are employed to predict spatial heterogeneities in the pressure field in a specific patient's coronary artery. The results, in terms of pressure profiles, are compared across four different physiological scenarios.*

Keywords: hemodynamics, reduced-order models, computational fluid dynamics, ANSYS

1. INTRODUCTION

In contemporary times, Computational Fluid Dynamics (CFD) methods are frequently employed to solve governing equations such as the Navier-Stokes equations and continuity equations, enabling a better understanding of coronary flow (Pandey, 2020). Additionally, higher-order model solutions using CFD are utilized to comprehend the pathophysiology of coronary disease development and progression, potentially reducing the cost, time, and risk of clinical trials (Shi et al., 2011, 2016, 2018a, 2018b, 2021). The following paragraphs provide a brief overview of literature published over the past two decades.

Ku et al. (1997), in their review, suggest that the slope of the velocity profile may result in pockets where the wall shear stress direction oscillates, potentially leading to atherosclerosis. Very high shear stress near a stenosis throat can activate platelets, leading to thrombosis. Using ventricular pressure in three-dimensional epicardial coronary arteries, Kim et al. (2010) developed a hybrid higher-order finite element (FE) method associated with lower-order models to predict coronary flow and pressure. Compared to literature data, the calculated coronary flow and pressure waveforms were realistic.

According to Sankaran et al. (2012), using CT images and non-invasive clinical measurements, a computational framework was developed to model and simulate blood flow in patients with coronary artery bypass grafts. The influence of graft shape on local hemodynamics and global circulation dynamics was assessed by systematically parameterizing graft geometry. In Chaichana et al.'s study (2012), left coronary artery plaques resulted in significant increases in pressure gradients and reduced flow velocities. They argue that coronary plaques directly influence hemodynamic environment, and wall shear stress is similar between models based on non-Newtonian and Newtonian theories.

Tu et al. (2013) explain that the velocity of a coronary aneurysm was accurately predicted under physiological flow conditions in a realistic coronary aneurysm anatomy. The velocity difference between Phase-Contrast Magnetic Resonance Imaging (PCMRI) and CFD was quantifiable and proportional to flow velocity. Wall shear stress differences between deformable and rigid walls were evaluated. Several factors influence wall shear stress and wall pressure gradient in coronary artery hemodynamic analyses, including branch curvature and angle, as well as tortuosity, which can negatively affect coronary perfusion pressure and atherosclerotic lesions, as explained by Vorobtsova and Morris (2015,

2016). Conversely, tortuous arteries exhibit higher wall shear stress, suggesting that coronary tortuosity may play a significant role in slowing atherosclerosis progression (Yang, 2017). On this note, Lee et al. (2019) conducted an assessment of diagnostic characteristics of computational fractional flow reserve (FFR) derived from coronary CT angiography. Sensitivity and specificity of their results were quantified. Supporting this, Freidoonimehr and Kandangwa (2022a, 2022b) recently concluded that it was possible to overlook temporal and spatial variations in coronary arteries while providing a reliable estimate of hemodynamic parameters such as pressure drop, wall shear stress values, and oscillatory shear index values.

It is also valid to mention the works of Jung (2006a, 2006b) and Gidaspow and Huang (2009) using multiphase theory to describe some phenomena in coronary blood flow. Jung (2006a, 2006b) used a three-dimensional non-Newtonian transient multiphase model to solve flow in an idealized curved section of the human coronary artery. In their study, red blood cells were correctly predicted to accumulate on the inner curve. However, their biphasic non-Newtonian viscosity models predict higher shear thinning than monophasic non-Newtonian models, leading to lower oscillatory wall shear stress (OWSS) on inner curves. Additionally, Bulant (2017) directly compared predictions of CFD models based on computed tomography angiography (CCTA) and intravascular ultrasound (IVUS) acquisition protocols. His conclusions were that coronary geometry provided by CCTA overestimated pressure drops, due to substantial lumen area underestimation in coronary vessels, leading to overestimation of FFR values. Furthermore, Gidaspow and Huang (2009) presented a multiphase kinetic model of pulsatile flow in a realistic main branch of the right coronary artery. The model correctly estimated red blood cell viscosity and migration away from vessel walls. Due to this, the maximum curvature inner area exhibited the highest wall shear stress and wall shear stress gradient, possibly indicating atherosclerosis.

Despite being integrated into clinical workflows (Taylor et al., 2013; Lee et al., 2019), the use of CFD solutions can be financially prohibitive for less affluent healthcare systems today. Shi et al. (2011) found that, to reduce computational costs, lower-order models based on simplified representations of the heart and blood vessels (0D, 1D) can be effective in clinical settings. In 0D models, hemodynamic variables (pressure and volumetric flow) are assumed to be uniformly distributed at any given time, while in 1D models, these variables are assumed to depend on a coordinate in space. In Blanco (2018), the authors compared the predictive value of 1D and 3D models, showing excellent agreement between these models in terms of FFR. However, it is also known that 1D models lack definition of velocity and pressure fields in 3D space.

In this context, aiming to reduce computational costs in hemodynamic simulations, medium-fidelity models can be positioned as an interesting alternative between higher-order models (3D CFD solutions) and lower-order models (0D and 1D). Recently, Mansilla Alvarez et al. (2022) developed a medium-fidelity model (TEPEM) and addressed its reliability in simulating a collection of coronary arteries. A comparison of TEPEM results with a full-order FEM model produced a 1% error for FFR and 5% for WSS. Based on Mansilla Alvarez et al.'s findings (2022), the objective of this study is to contrast TEPEM model results with those of a full-order model solution produced by an FVM solver available in a commercial CFD tool (ANSYS Fluent 21R1).

2. METHODOLOGY

The coronary flow in the present work is modeled using steady-state Navier-Stokes equations for an incompressible Newtonian fluid

$$\rho(u \cdot \nabla)u = -\nabla p + \mu\nabla^2 u \tag{1}$$

In the above equations, $\mathbf{u}$ is the velocity vector field and ρ is the scalar pressure field. Constant values for density ρ and viscosity μ were used. The numerical methodology for obtaining the solution of the above equation using the FVM method can be found for instance in Maliska (2023). For the TEPEM numerical methodology, a primer can be found in Alvarez et all (2016)

Regarding the simulations presented in this work, the ANSYS Design Explorer 2021R simulator, considered high fidelity, and the TEPEM - Transversally Enriched Pipe Element Method - as a medium-fidelity strategy were utilized. FLUENT is a computational simulation software developed by ANSYS, widely used in fluid analysis and heat transfer, which employs the finite volume method as a foundation for solving conservation equations in computational fluid dynamics (CFD) problems. The finite volume method is a numerical technique for solving partial differential equations that describe fluid behavior. This method divides the domain of interest into finite cells or volumes, discretizing the equations in each of these cells. It approximates the derivatives of variables based on average values within each cell, calculating mass, energy, and momentum flow rates (ANSYS FLUENT Theory Guide 2011).

In this context, to perform simulations in ANSYS, the steady-state assumption with laminar flow was adopted for the geometries. The relaxation factors used were 1, 1, 0.5, and 0.5, corresponding to density, body forces, momentum, and pressure, respectively. Blood parameters were defined with a viscosity of 0.004 kg/(m-s) and a density of 1040 kg/m³. These simulations were executed using the coupled algorithm, which involves the iteration and coupling of different components or processes instead of treating each component separately. This approach considers the mutual influence

between components, allowing for a more accurate and realistic resolution. For solid fill elements, polyhedral meshes with flat faces were used instead of rectangular or square faces. These faces adapt more easily to geometric features, resulting in better outcomes.

On the other hand, TEPEM is a finite element-based strategy specifically designed for simulating blood flow in medium and large vascular networks. This method involves enriching finite elements to more accurately capture transverse predictive features, assuming that behavior in this direction is accurately described by high-order polynomials. TEPEM has been extensively tested in previous works, such as (Mansilla Alvarez et al. 2017), and is implemented in an internal solver framework. Model parameters, viscosity, and density, are the same as described in the last paragraph, while algebraic equation systems were solved using the same iterative GMRES method with implicit Euler backward time discretization and Picard iterations for nonlinear convective terms.

3. RESULTS AND DISCUSSION

To test the differences between TEPEM and FLUENT predictions, a single geometric model was employed in four different physiological scenarios. The geometric model corresponds to a specific right coronary artery of the patient, segmented from a set of coronary CT angiography (CCTA) medical imaging data. The geometry was divided into 141,251 cells for high-fidelity simulation and 12,816 elements for medium-fidelity simulation. As boundary conditions, the resting flow (Q = 1.44 cm³/s) is split and applied at each distal boundary (outlet boundary conditions), while the zero Neumann condition is considered for the proximal boundary. To simulate different physiological scenarios, the total flow is scaled by a factor denoted by CFR (coronary flow reserve) with values CFR = {2, 3, 4, 5}. This approach simulates various hyperemic conditions, emulating the physical scenario where blood flow-related quantities for arterial functionality measurement are assessed.

Subsequently, comparisons between FLUENT and TEPEM in this right coronary artery geometry were presented. To better appreciate the details, four regions of interest were selected: a proximal region (a), two bifurcations (b) and (c), and a distal region (d). In Figure 1, the pressure field predicted by FLUENT and TEPEM for the resting scenario was compared. The figure in the left panel shows the pressure field provided by the FLUENT solver, where the pressure is in Pascal units (Pa). Additionally, in the same figure, the differences in the four selected regions are highlighted. For the resting case, differences between the two strategies are minimal, with a slight difference in pressure distribution in region (b), the first bifurcation. However, these differences are not significant if the goal is to focus on pressure drop or identify regions of high or low-pressure values. Both tubular regions, indicated as (a) and (b), show good agreement between ANSYS and TEPEM, suggesting that the larger differences (located at the junctions) are due to the complexity of the flow in these regions.

.

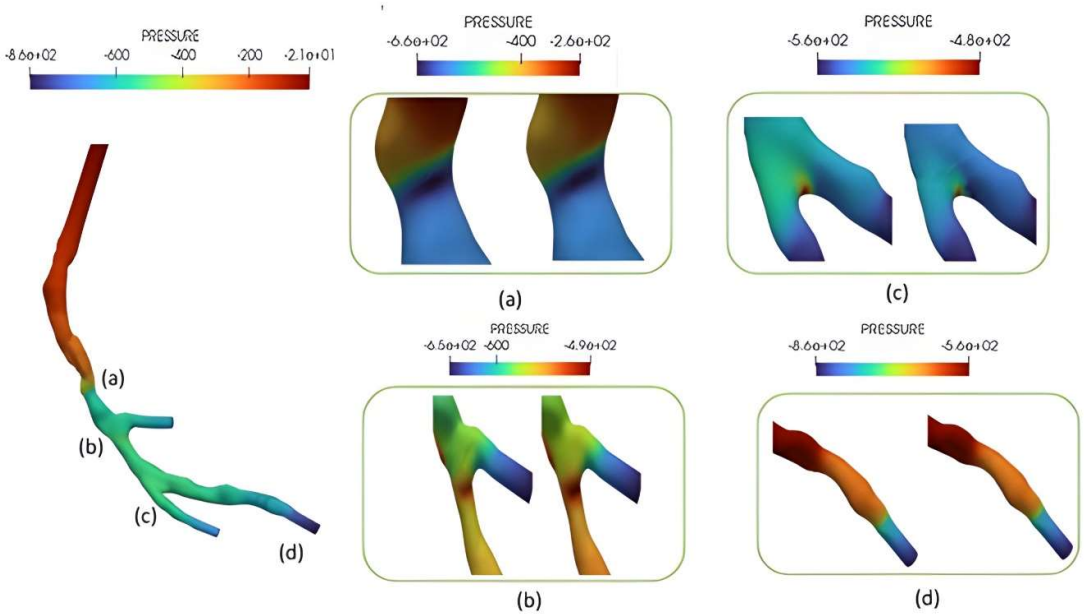

Figure 1 - Left: Pressure distribution obtained with FLUENT for the at-rest scenario (CFR = 1). At each panel, the comparison between FLUENT (left) and TEPEM (right) in four different regions is presented.

In Figure 2, in the left panel, the pressure field provided by the FLUENT solver for CFR=2 is shown. In this representation, the pressure unit is "Pa" (Pascal). Additionally, in the same figure, differences in the four selected regions are highlighted. Under CFR=2 conditions, the differences between the two configurations are minimal, with only a small discrepancy in pressure distribution in Figure 2.(c), the second bifurcation. In FLUENT, a larger area of relatively lower pressures was observed compared to TEPEM, possibly caused by an increased flow rate.

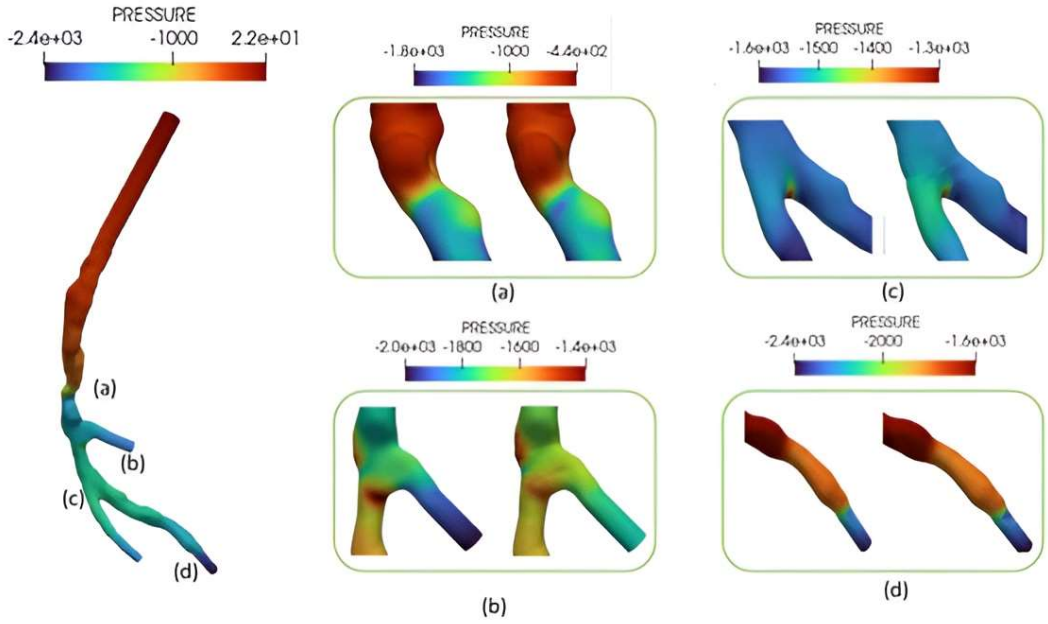

Figure 2 - Left: Pressure distribution obtained with FLUENT for the scenario with (CFR = 2). At each panel, the comparison between FLUENT and TEPEM in four different regions is presented.

In Figure 3, on the left, the pressure field established by FLUENT for CFR=3 is highlighted. In this execution, the pressure unit is "Pa" (Pascal). Additionally, in the same figure, differences in the four selected regions are displayed. A difference in pressure values between FLUENT and TEPEM was observed in Figure 3.(b), and despite this discrepancy, the regions where pressure variations occur in each panel are practically in the same locations. In Figure 3.(c), an increase in the area of higher pressures was noted compared to Figure 2.(c), possibly caused by the increased flow rate in this simulation.

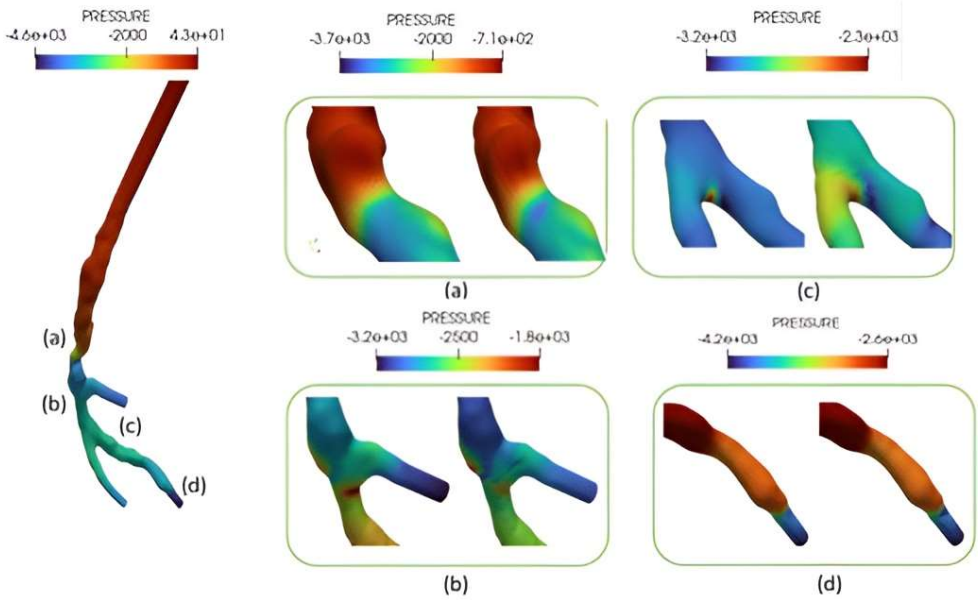

Figure 3 - Left: Pressure distribution obtained with FLUENT for the scenario with (CFR = 3). At each panel, the comparison between FLUENT and TEPEM in four different regions is presented.

Figure 4, in the left panel, highlights the pressure field obtained by FLUENT. In this case, the pressure unit is "Pa" (Pascal). Furthermore, in the same figure, differences in the four selected regions are displayed. It is inferred that in Figures 4.(b) and 4.(c), corresponding to the first and second bifurcations, there is an increase in the area of higher pressures, likely induced by the increased velocity. However, it is worth noting that, in both simulations, the areas of pressure variations occur in the same locations in each compared image.

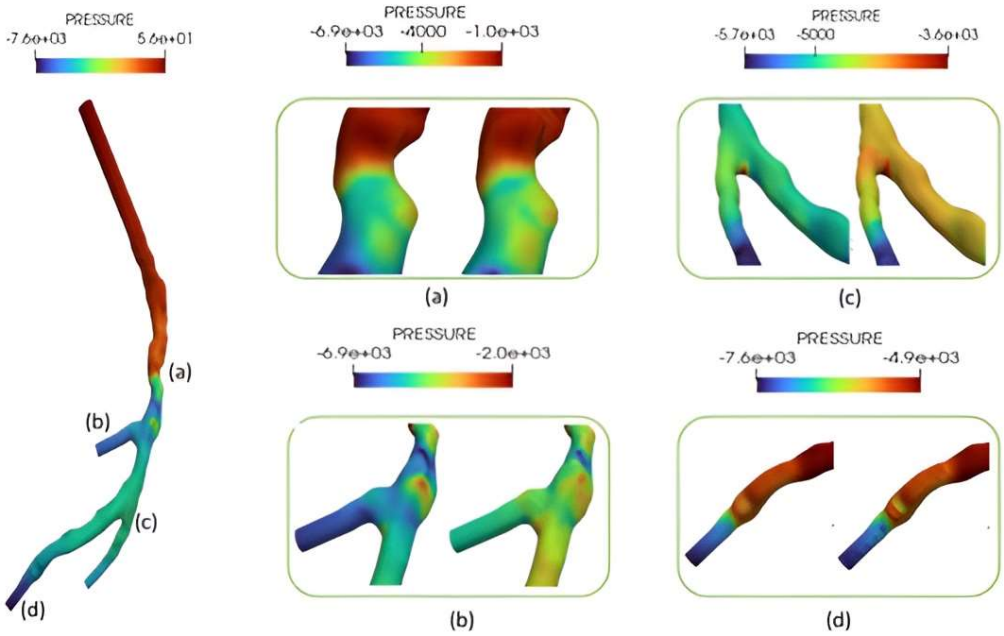

Figure 4 - Left: Pressure distribution obtained with the FLUENT for the scenario with CFR = 4. At each panel, the comparison between FLUENT and TEPEM in four different regions is presented.

In general, in panels "a," it was observed that the pressure is higher in the anterior part before the narrowing of the artery. In panels "b," an increase in pressure was noted in the left vessel at the first bifurcation. Regarding panels "c," a high-pressure point in the center of the wall of the second bifurcation can be highlighted. As for panel "d," there is also an increase in pressure due to the narrowing of the artery.

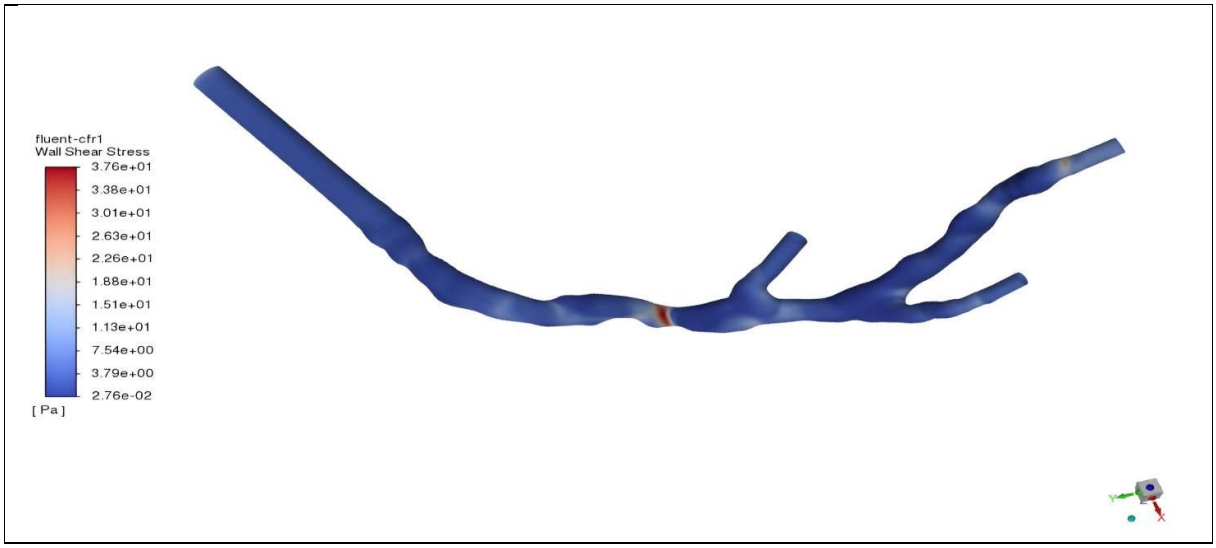

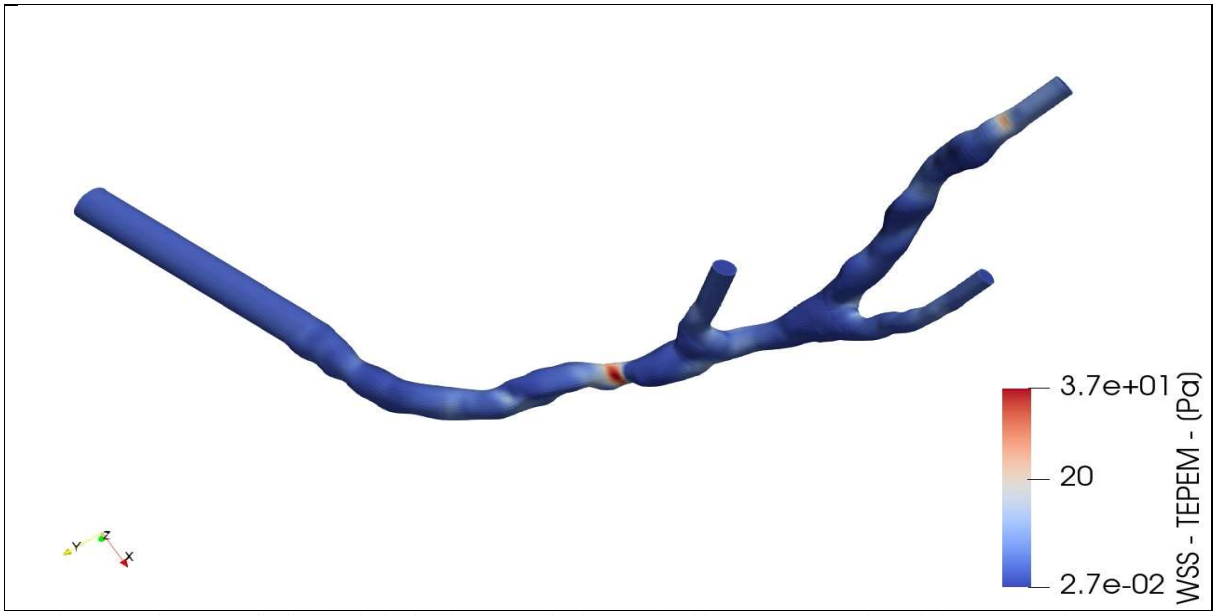

Figure 5 - Left: Pressure distribution obtained with FLUENT for the scenario with (CFR = 1). At each panel, the comparison between FLUENT and TEPEM in different regions is presented for wall shear stress,

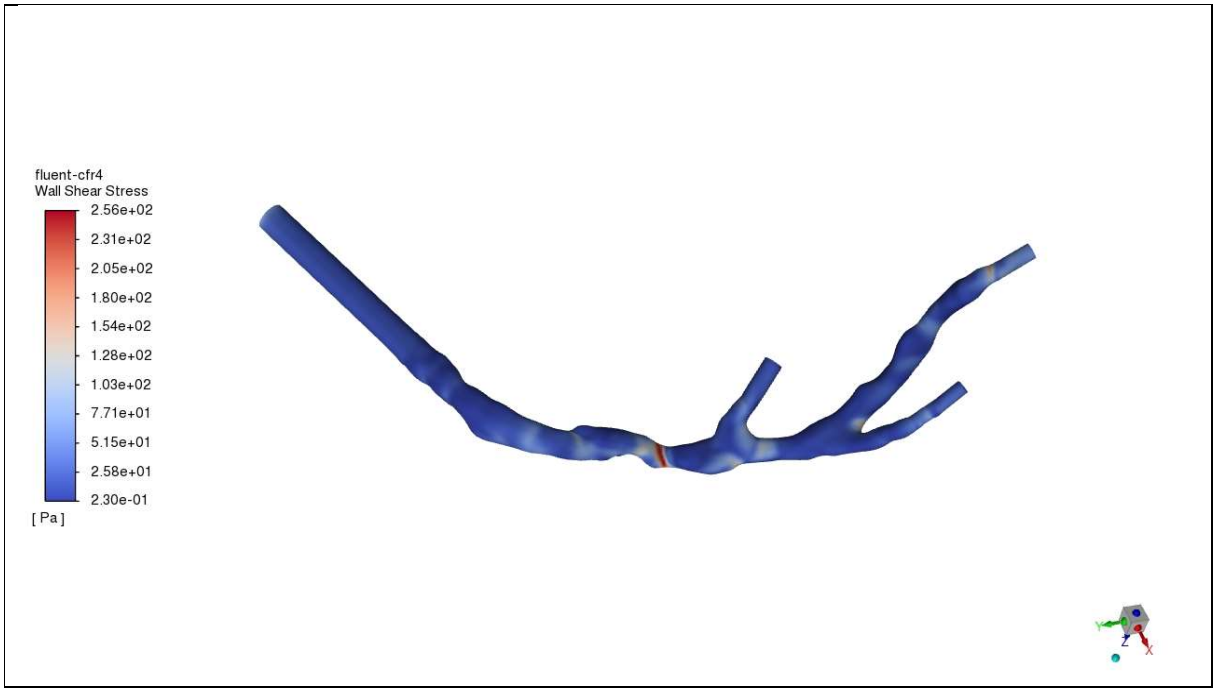

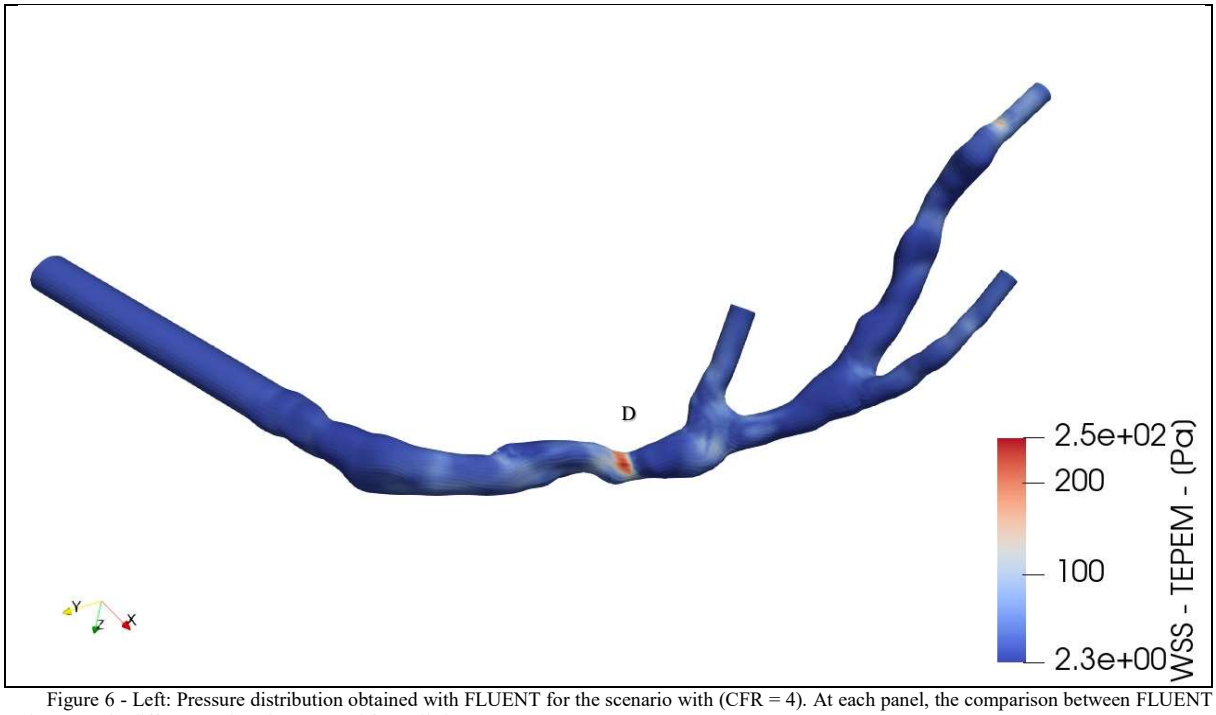

Figure 6 - Left: Pressure distribution obtained with FLUENT for the scenario with (CFR = 4). At each panel, the comparison between FLUENT and TEPEM in different regions is presented for wall shear stress,

In both figures (5) and (6), we observe similarity in measurements and locations of higher stress, marked with the letter (d), where an aneurysm is present. This consistency reinforces the validity and reliability of the conclusions, indicating that the results are not mere coincidences but rather consistent patterns that will lead to further studies in the future.

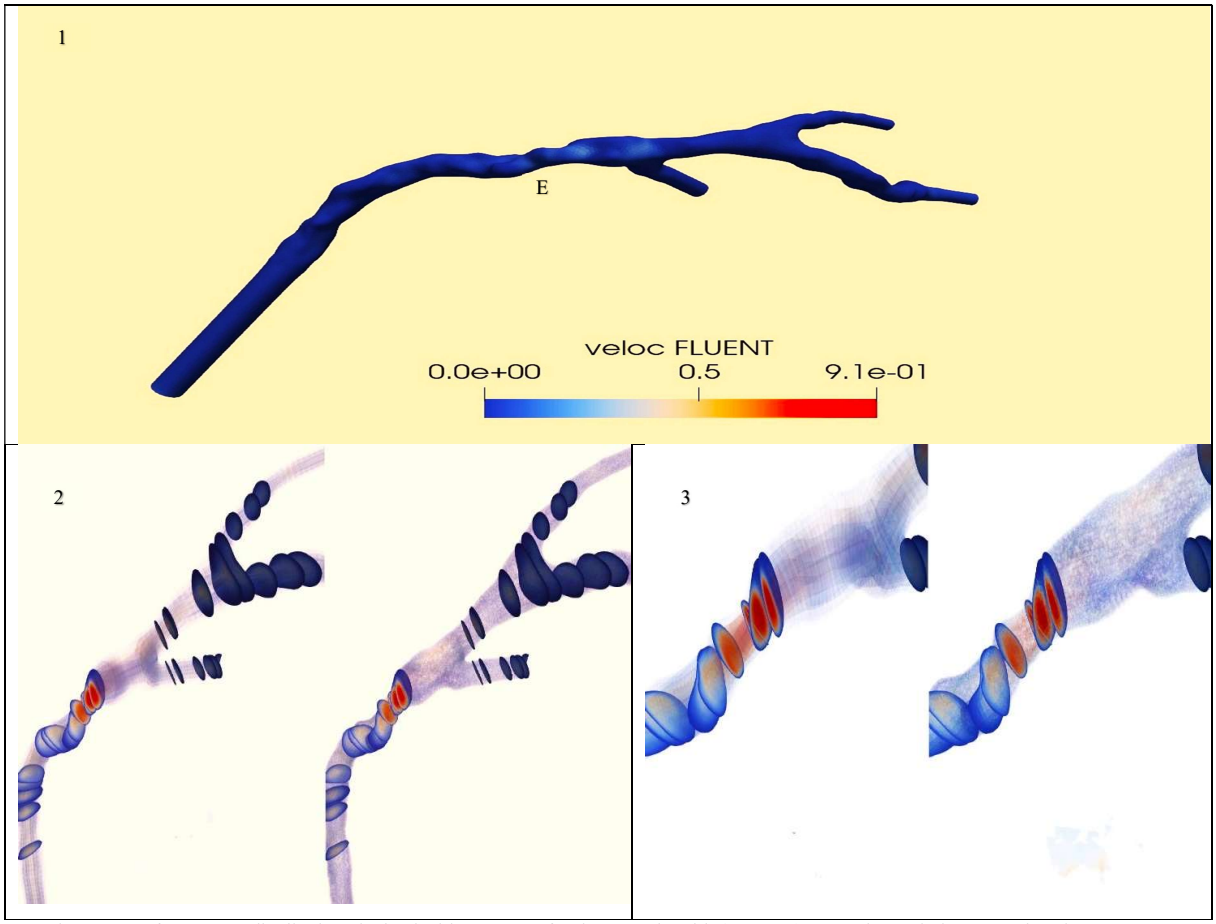

Figure 7 - Left: Pressure distribution obtained with FLUENT for the scenario with (CFR = 1). At each panel, the comparison between FLUENT (left) and TEPEM (right) in different regions is presented for Profiles of velocity In the charts" or "In the frames (2) e (3).

In both simulations, a sharp increase in velocity is evident at the location of the artery aneurysm, marked by the letter (E). This constriction in the fluid passage area leads to a notable acceleration in the outlet velocity. The consistency observed in both simulations not only highlights the coincidental nature of these results but also emphasizes the presence of coherent patterns. This observation may lead to a deeper exploration of fluid flow dynamics in the context of arterial aneurysms, promoting a deeper understanding of the underlying mechanisms at play.

4. CONCLUSÃO

A higher CFR (Total Flow) correlates with a higher Reynolds number, resulting in increased flow velocity and greater complexity in flow patterns. Remarkably, a detailed examination of the figures, especially in Figure 4, reveals the most significant disparities in vascular bifurcations, where intricate phenomena such as recirculation and potential turbulence manifest. In the proximal and distal regions, similarities in pressure drop emerge between the high-fidelity model (using the Finite Volume Method, FVM) and the medium-fidelity numerical approach (employing the Transversally Enriched Pipe Element Method, TEPEM). This similarity arises from the complex nature of fluid flow in vascular bifurcations, leading to notable variations in pressure distributions and explaining the observed differences between high and medium-fidelity models.

Consistency and strong agreement characterize the results of both simulations, instilling confidence in the accuracy of the medium-fidelity model compared to the high-fidelity model. Particularly crucial in experimental research, where replication is fundamental to establishing the validity of findings, these preliminary results lay the groundwork for ongoing critical analysis of the study methodology and consulted sources. Furthermore, they prompt consideration of additional comparative investigations to yield more comprehensive and reliable conclusions. In this context, it is

emphasized that the high-fidelity model, employing the Finite Volume Method (FVM), excels in providing detailed predictions, serving as a benchmark for performance comparison with the medium-fidelity numerical approach (TEPEM), strategically positioned between low and high-fidelity models to simulate fluid flow in tubular domains.

5. REFERENCES

Alvarez, L. Mansilla, Blanco, Pablo, Bulant, C. D. Enzo, Veneziani, Alessandro, Feijóo, Raul, 2016. "transversally enriched pipe element method (TEPEM): An effective numerical approach for blood flow modeling" . International Journal for Numerical methods in Biomedical Engineering.

Chaichana, T., Sun, Z., Jewkes, J., 2012. "Computational fluid dynamics analysis of the effect of plaques in the left coronary artery". *Computational and Mathematical Methods in Medicine*, Vol. 2012, p. 504367.

Freidoonimehr, N., Chin, R., Zander, A., Arjomandi, M., 2022a. "A review on the effect of temporal geometric variations of the coronary arteries on the wall shear stress and pressure drop". *Journal of Biomechanical Engineering*, Vol. 144, Num. 1, p. 010801.

Gidaspow, D., Huang, J., 2009. "Kinetic theory based model for blood flow and its viscosity". *Annals of biomedical engineering*, Vol. 37, pp. 1534-1545.

Gray, R., A., Pathmanathan, P., 2018a. "Patient-specific cardiovascular computational modeling: diversity of personalization and challenges". *Journal of Cardiovascular Translational Research*, Vol. 11, pp. 80-88.

Hashemi, J., Patel, B., Chatzizisis, Y. S., Kassab, G. S., 2002. "Real time reduced order model for angiography fractional flow reserve". *Computer Methods and Programs in Biomedicine*, Vol. 216, p. 106674.

Jung, J., Hassanein, A., Lyczkowski, R. W., 2006. "Hemodynamic computation using multiphase flow dynamics in a right coronary artery". *Annals of Biomedical Engineering*, Vol. 34, pp. 393-407.

Jung, J., Lyczkowski, R. W., Panchal, C. B., Hassanein, A., 2006. "Multiphase hemodynamic simulation of pulsatile flow in a coronary artery". *Journal of Biomechanics*, Vol. 39, Num. 11, pp. 2064-2073.

Kandangwa, P., Tprri, R., Getehouse, P. D., Sherwin, S. J., Weinberg, P. D., 2022b. "Influence of right coronary artery motion, flow pulsatility and non-Newtonian rheology on wall shear stress metrics". *Frontiers in Bioengineering and Biotechnology*, Vol. 10, p. 1336, 2022b.

Kim, H. J., Vignon-Clementel, I. E., Coogan, J. S., Figueroa, C. A., Jansen, K. E., Taylor, C. A., 2010. "Patient-specific modeling of blood flow and pressure in human coronary arteries". *Annals of Biomedical Engineering*, Vol. 38, pp. 3195-3209.

Ku, D. N., 1997. "Blood flow in arteries". *Annual Review of Fluid Mechanics*, Vol. 29, Num. 1, pp. 399-434.

Lee, B.-K., 2011. "Computational fluid dynamics in cardiovascular disease". *Korean Circulation Journal*, Vol. 41, Num. 8, pp. 423-430.

Lee, J. M., Choi, G., Koo, B-K., Hwang, D., Park, J., Zhang, J., Kim, K-J., Tong, Y., Grady, L., Doh, J-H., Nam, C-W., Shin, E-S., Cho, Y-S., Choi, S-Y., Chun, E. J., Choi, J-H., Norgaard, B. L., Christiansen, E. H., Niemen, K., Otake, H., Penicka, M., Bruyne. B., Kubo, T., Akasaka, T., Narula, J., Douglas, P. S., Taylor, C. A., Kim, H-S., 2019. "Identification of high-risk plaques destined to cause acute coronary syndrome using coronary computed tomographic angiography and computational fluid dynamics". *Cardiovascular Imaging"*, Vol. 12, Num. 6, pp. 1032-1043.

Liu, G., Wu, J., Ghista, D. N., Huang, W., Wong, K. K. L., 2015. "Hemodynamic characterization of transient blood flow in right coronary arteries with varying curvature and side-branch bifurcation angles". *Computers in Biology and Medicine*, Vol. 64, pp. 117-126.

Mansilla Alvarez, L. A., Bulant, C. A., Ares, G. D., Feijó, R. A., Blanco, P. J., 2022. "Feasibility of coronary blood flow simulations using mid-fidelity numeric and geometric models". *Biomechanics and Modeling in Mechanobiology*, Vol. 21, Num. 1, pp. 317-334.

Maliska, C. R. 2023. Fundamentals of Computational Fluid Dynamics: The Finite Volume Method (Vol 135). Springer Nature.

Morris, P. D., Narracott, A., Tengg-Kobligk, H. v., Soto, D. A. S., Hsiao, S., Lungu, A., Evans, P., Bressloff, N., Lawford, P. V., Hose, D. R., Gunn, J. P., 2016. "Computational fluid dynamics modelling in cardiovascular medicine". *Heart*, Vol. 102, Num. 1, pp. 18-28.

Pandey, R., Kumar, M., Majdoubi, J., Rahimi-Gorji, M., Srivastav, V. K., 2020. "A review study on blood in human coronary artery: Numerical approach". *Computer Methods and Programs in Biomedicine*, Vol. 187, p. 105243.

Sankaran, S., Esmaily Moghadam, M., Kahn, A. M., Tseng, E. E., Guccione, J. M., Marsden, A. L., 2012. "Patient-specific multiscale modeling of blood flow for coronary artery bypass graft surgery". *Annals of Biomedical Engineering*, Vol. 40, pp. 2228-2242.

Shi, Y., Lawford, P., Hose, R., 2011. "Review of zero-D and 1-D models of blood flow in the cardiovascular system". *Biomedical Engineering Online*, Vol. 10, pp. 1-38.

Taroco, E. O., Blanco, P. J., Feijoo, R. A. (2020). Introduction to the Variational Formulation in Mechanics: Fundamentals and Applications. John Wiley & Sons.

Taylor, C. A., Fonte, T. A., Min, J. K., 2013. "Computational fluid dynamics applied to cardiac computed tomography for noninvasive quantification of fractional flow reserve: Scientific basis". *J. Amer. Coll. Cardiol.*, Vol. 1, pp. 2233-2241.

Tu, S., Pyxaras, S. A., Li, Y., Barbato, E., Reiber, J. H. C., Wijins, W., 2013. "In vivo flow simulation at coronary bifurcation reconstructed by fusion of 3-dimensional X-ray angiography and optical coherence tomography". *Circulation: Cardiovascular Interventions*, Vol. 6, Num. 2, pp. e15-e17.

Vardhan, M., Randles, A., 2021. "Application of physics-based flow models in cardiovascular medicine: Current practices and challenges". *Biophysics Reviews*, Vol. 2, Num. 1, p. 11302.

Vorobtsova, N., Chiastra, C., Stremler, M. A., Sane, D. C., Migliavacca, F., Vlachos, P., 2016. "Effects of vessel tortuosity on coronary hemodynamics: an idealized and patient-specific computational study". *Annals of Biomedical Engineering"*, Vol. 44, pp. 2228-2239.

Yang, L., Xiuxian, L., Zhi-Yong, L., Jiayi, T., Yi, F., Genshan, M., Chengxing, S., Naifeng, L., 2017. "Impact of coronary tortuosity on coronary pressure and wall shear stress: an experimental study". *Molecular & Cellular Biomechanics*, Vol. 14, Num. 4, p. 213.

Zhong, L., Zhang, J-M., Su, B., Tan, R. S., Allen, J. C., Kassab, G. S., 2018b. "Application of patient-specific computational fluid dynamics in coronary and intra-cardiac flow simulations: Challenges and opportunities". *Frontiers in Physiology*, Vol. 9, p. 742.

SHI, Yubing; LAWFORD, Patricia; HOSE, Rodney. Review of zero-D and 1-D models of blood flow in the cardiovascular system. **Biomedical engineering online**, v. 10, p. 1-38, 2011.